Search for new phenomena in events with a monojet and large missing transverse momentum at the LHC using the ATLAS detector

Mario Martínez[1,a]

ICREA/Institut de Física d'Altes Energies, Bellaterra, Barcelona 08193, Spain.

(*on behalf of the ATLAS Collaboration*)

Abstract. We report preliminary results on a search for new phenomena in an event sample with monojets and large missing transverse momentum in the final state. The analysis uses 1.00 fb^{-1} of data collected in 2011 with the ATLAS detector [1]. Good agreement is observed between the number of events in data and the Standard Model predictions. The results are translated into improved limits on a model with Large Extra Dimensions.

1 Introduction

The search for new physics in events with a high transverse energy jet and large missing transverse energy constitutes one the simplest and most striking signatures that can be observed at a hadron collider. Different theoretical models for physics beyond the standard model (SM) predict the presence of *monojet* signatures in the final state like, for example, Large Extra Dimension (LED) scenarios [2].

In the Arkani-Hamed, Dimopoulos, and Dvali (ADD) LED model considered in this analysis, the four-dimensional Planck scale, M_{Pl}, is related to the fundamental $4 + n$-dimensional Planck scale, M_D, by ${M_{Pl}}^2 \sim {M_D}^{2+n} R^n$, where n and R are the number and compactification radius of the extra dimensions, respectively. An appropriate choice of R for a given n allows for a value of M_D close to the electroweak scale. The compactification of the extra spatial dimensions results in a Kaluza-Klein tower of massive graviton modes. These graviton modes are produced in association with a jet and do not interact with the detector, which results in a monojet signature in the final state. For the production of the graviton mass modes in the ADD scenario, a low-energy effective field theory, governed by the energy scale M_D, is used.

2 Event Selection

The data sample considered in this analysis was collected with ATLAS tracking detectors, calorimeters, muon chambers, and magnets operational, and corresponds to a total integrated luminosity of 1.00 fb^{-1}. The data were selected online using a trigger logic that selects events with missing transverse momentum $E_{\mathrm{T}}^{\mathrm{miss}}$ above 60 GeV, which is more than 98% efficient for $E_{\mathrm{T}}^{\mathrm{miss}} > 120$ GeV, as determined using an unbiased data sample with muons in the final state.

The offline event selection criteria applied follow closely those in Ref. [3], which defined two separate LowPt and HighPt set of requirements with the aim to maintain the sensitivity to a varity of models for new phenomena. With the increase in statistics, a new veryHighPt set of requirements is now defined to improve the sensitivity to signals of new phenomena at very large transverse momenta. The following event selection criteria are applied:

- Events are required to have a reconstructed primary vertex. This rejects beam-related backgrounds and cosmic rays.
- Events are rejected if they contain any jet with $p_{\mathrm{T}} > 20$ GeV and $|\eta| < 4.5$ that present anomalous charged fraction f_{ch} [1], electromagnetic fraction f_{em} in the calorimeter, or timing (as determined from the energy deposits of the jet constituents) inconsistent with originating from a proton-proton collision, and most likely produced by beam-related backgrounds and cosmic rays. In addition, the highest p_{T} jet selected (see below) is required to have $f_{\mathrm{ch}} > 0.02$ and $f_{\mathrm{em}} > 0.1$. Additional requirements are applied to suppress coherent noise and electronic noise bursts in the calorimeter producing anomalous energy deposits.
- During 2011, part of the data suffered from the presence of a hole in the electromagnetic calorimeter coverage in the region $0 < \eta < 1.45$ and $0.788 < \phi < -0.592$, which affected the readout of two of the LAr calorimeter layers. The effect of the reduced calorimeter response was studied and resulted into a slightly modified event selection. A fiducial requirement is applied to the jets and electrons in the final state to avoid any bias in the analysis. Events are rejected if there is any jet with p_{T} above 20 GeV or an identified electron in the final state such that their distance to the edges of the calorimeter affected region in $\eta - \phi$ is less than 0.4 or 0.1, respectively.
- Events are required to have no identified electrons or muons in the final state.
- As in [3], the LowPt (HighPt) selection requires a jet with $p_{\mathrm{T}} > 120$ GeV ($p_{\mathrm{T}} > 250$ GeV) and $|\eta^{\mathrm{jet}}| < 2$ in the final state, and $E_{\mathrm{T}}^{\mathrm{miss}} > 120$ GeV ($E_{\mathrm{T}}^{\mathrm{miss}} > 220$ GeV). Events with a second leading jet p_{T} above 30 GeV (60 GeV) in the region $|\eta| < 4.5$ are rejected. For the HighPt selection, the p_{T} of the third leading jet

[a] e-mail: mmp@ifae.es

must be less than 30 GeV, and an additional requirement on the azimuthal separation $\Delta\phi(\text{jet}, E_{\text{T}}^{\text{miss}}) > 0.5$ between the $E_{\text{T}}^{\text{miss}}$ and the direction of the second leading jet is required, that reduces the QCD background contribution where the large $E_{\text{T}}^{\text{miss}}$ originates from the mis-measurement of the second-leading jet p_{T}.
– A new veryHighPt selection is defined with the same requirements as in the HighPt region, but with thresholds on the leading jet p_{T} and $E_{\text{T}}^{\text{miss}}$ increased up to 350 GeV and 300 GeV, respectively.

A total of 15740, 965 and 167 events are observed in the LowPt, HighPt and veryHighPt regions, respectively.

3 Background estimation

The expected background to the monojet signature is dominated by $Z\ (\rightarrow \nu\bar{\nu})$+jets and W+jets production, and includes contributions from $Z/\gamma^*(\rightarrow \ell^+\ell^-)$+jets ($\ell = e, \mu, \tau$), multi-jets, $t\bar{t}$, and γ+jets processes. The W/Z plus jets backgrounds are estimated using Monte Carlo (MC) event samples normalized using data in control regions. The remaining SM backgrounds from $t\bar{t}$ and γ+jets are determined using simulated samples, while the multi-jets background contribution is extracted from data. Finally, the potential contributions from beam-related background and cosmics rays are estimated using data.

3.1 Electroweak background

As explained in [3], control samples in data, orthogonal to the signal regions, with identified electrons or muons in the final state and with the same requirements on the jet p_{T}, subleading jet vetoes, and $E_{\text{T}}^{\text{miss}}$, are employed to determine the normalization of the electroweak backgrounds from data. This reduces significantly the relatively large theoretical and experimental systematic uncertainties associated to purely MC-based predictions. The muon control sample is used to normalize the $W(\rightarrow \mu\nu)$+jets, $Z\ (\rightarrow \nu\bar{\nu})$+jets, and $Z/\gamma^*(\rightarrow \mu^+\mu^-)$+jets MC predictions. Similarly, the electron sample is employed to determine the normalization of the $W(\rightarrow e\nu)$+jets, $Z/\gamma^*(\rightarrow e^+e^-)$+jets, and $W(\rightarrow \tau\nu)$+jets MC predictions.

3.2 Multi-jets background

The multi-jets background with large $E_{\text{T}}^{\text{miss}}$ originates mainly from the misreconstruction of the energy of a jet in the calorimeters, which goes below the required threshold, resulting in a monojet signature. In such events, the $E_{\text{T}}^{\text{miss}}$ direction will generally be aligned with the second-leading jet in the event. To estimate this background, jets-enriched data control samples are defined using the LowPt, HighPt, and veryHighPt selections without the veto on the second-leading jet p_{T} and requiring $\Delta\phi(jet2 - E_{\text{T}}^{\text{miss}}) < 0.5$. Events with more than two jets with p_{T} above 30 GeV are excluded. The measured p_{T} distribution of the second-leading jet in the multi-jets enriched control samples ($\Delta\phi(jet2 - E_{\text{T}}^{\text{miss}}) < 0.5$) are used to estimate the multi-jets background in the analyses. The number of multi-jets background events is obtained from a linear extrapolation below the threshold of $p_{\text{T}} < 30$ GeV ($p_{\text{T}} < 60$ GeV) for the LowPt (HighPt and veryHighPt) region.

3.3 Non-collision background

The contribution of non-collision backgrounds to the selected monojet samples from cosmics rays, overlaps between background events and genuine proton-proton collisions, and from beam-halo muons are estimated using events registered in empty and unpaired proton bunches in the collider that fulfill the event selection criteria, and a beam-halo tagger. The latter combines information from the muon chambers and the timing of calorimeter clusters.

The expected background predictions are summarized in Table 1 for the LowPt, HighPt, and veryHighPt selections. Good agreement is observed between the data and the SM predictions in all cases.

	Background Predictions ± (stat.) ± (syst.)		
	LowPt Selection	HighPt Selection	veryHighPt selection
$Z\ (\rightarrow \nu\bar{\nu})$+jets	7700 ± 90 ± 400	610 ± 27 ± 47	124 ± 12 ± 15
$W(\rightarrow \tau\nu)$+jets	3300 ± 90 ± 220	180 ± 16 ± 22	36 ± 7 ± 8
$W(\rightarrow e\nu)$+jets	1370 ± 60 ± 90	68 ± 10 ± 8	8 ± 1 ± 2
$W(\rightarrow \mu\nu)$+jets	1890 ± 70 ± 100	113 ± 14 ± 9	18 ± 4 ± 2
Multi-jets	360 ± 20 ± 290	30 ± 6 ± 11	3 ± 2 ± 2
$Z/\gamma^*(\rightarrow \tau^+\tau^-)$+jets	59 ± 3 ± 4	2.0 ± 0.6 ± 0.2	-
$Z/\gamma^*(\rightarrow \mu^+\mu^-)$+jets	45 ± 3 ± 2	2.0 ± 0.6 ± 0.1	-
$t\bar{t}$	17 ± 1 ± 3	1.7 ± 0.3 ± 0.3	-
γ+jet	-	-	-
$Z/\gamma^*(\rightarrow e^+e^-)$+jets	-	-	-
Non-collision Background	370 ± 40 ± 170	8.0 ± 3.3 ± 4.1	4.0 ± 3.2 ± 2.1
Total Background	15100 ± 170 ± 680	1010 ± 37 ± 65	193 ± 15 ± 20
Events in Data (1.00 fb^{-1})	15740	965	167

Table 1. Number of observed events and predicted background events, including statistical and systematic uncertainties. The statistical uncertainties are due to limited MC statistics. The dominant systematic uncertainties come from the limited statistics in the data control regions. The systematic uncertainties on $W(\rightarrow \mu\nu)$+jets, $Z/\gamma^*(\rightarrow \mu^+\mu^-)$+jets, and $Z\ (\rightarrow \nu\bar{\nu})$+jets predictions are fully correlated. Similarly, the systematic uncertainties on $W(\rightarrow e\nu)$+jets, $W(\rightarrow \tau\nu)$+jets, and $Z/\gamma^*(\rightarrow \tau^+\tau^-)$+jets are fully correlated.

4 Results

Figure 1 shows the measured $E_{\text{T}}^{\text{miss}}$ distribution for the LowPt selection compared to the background predictions. For illustrative purposes, the Figure indicates the impact of two different ADD scenarios.

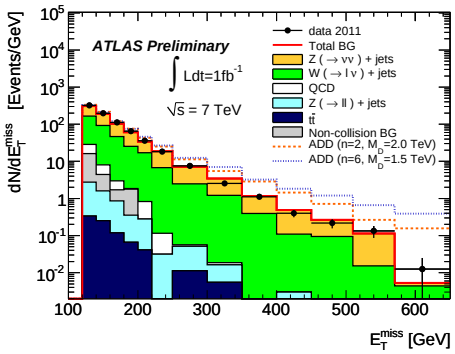

Fig. 1. Measured $E_{\text{T}}^{\text{miss}}$ distribution (black dots) in the LowPt region compared to the predictions for SM backgrounds (histograms). Only statistical uncertainties are considered. For illustrative purposes, the impact of two different ADD scenarios is included.

4.1 Model-independent limits on $\sigma\times$ Acceptance

The agreement between the data and the SM predictions for the total number of events in the different analyses is translated into model-independent 95% confidence level (CL) upper limits on the cross section times acceptance. The CL_s modified frequentist approach is used and the upper limits are computed considering the uncertainties on the background predictions (see Table 1) and a 4.5% uncertainty on the quoted integrated luminosity. The resulting 95% CL limits on cross section times acceptance for the LowPt, HighPt, and veryHighPt selections are 1.7 pb, 0.11 pb, and 0.035 pb, respectively.

The data are used to set new improved 95% CL upper limits on the parameters of the ADD LED model. MC simulated samples for the ADD LED model with different number of extra dimensions varying from 2 to 6 are generated using the PYTHIA program with CTEQ6.6 PDFs, and renormalization and factorization scales set to $\frac{1}{2}M_G^2 + p_T^2$, where M_G is the graviton mass and p_T denotes the transverse momentum of the recoiling parton. As already pointed out in [3], the effective theory used to compute the ADD cross sections remains valid only if the scales involved in the hard interaction are smaller than M_D. Otherwise, the predictions strongly depend on the unknown ultraviolet behavior of the theory.

Figure 2 shows the predicted ADD cross section times acceptance in the HighPt region as a function of M_D for 2 and 4 extra dimensions, where the band reflects the total uncertainty on the signal. For illustration purposes, the model-independent limit of 0.11 pb is included.

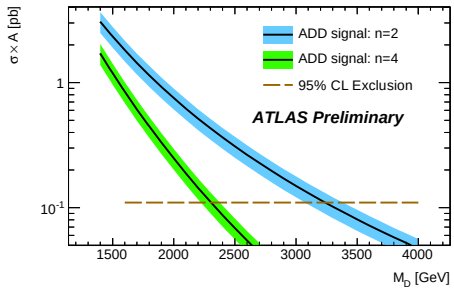

Fig. 2. Cross section times acceptance curves as a function of M_D predicted by the effective theory for 2 and 4 extra dimensions. The bands surrounding the curves reflect the systematic uncertainties on the predicted signal yields. The model-independent cross section times acceptance limit is shown as a dashed line for the HighPt region.

The simulation indicates that the detector effects reduce the expected signal yields, as determined at the particle level, by a factor 0.83 ± 0.01, approximately independent of M_D and n. This results into 95% CL cross section upper limits of 2.02 pb, 0.13 pb, and 0.045 pb for the LowPt, HighPt, and veryHighPt regions, respectively.

4.2 Lower limits on M_D

New improved 95% CL lower limits are set on the value of M_D as a function of the number of extra dimensions considered in the ADD LED model. The CL_s approach is used, including statistical and systematic uncertainties. The HighPt selection is used for the final results. It provides better expected limits than the ones obtained in the LowPt region, and the results are comparable with those for the veryHighPt region (mainly due to the rapid decrease of the signal cross section with increasing jet p_T and E_T^{miss}) but with a reduced sensitivity to the ultraviolet behavior of the theory [1]. Figure 3 presents the observed 95% CL lower limits on M_D as a function of the number of extra dimensions varying from 2 to 6, as determined by the HighPt selection. This analysis imposes 95% CL upper limits for the scale M_D that vary between 3.2 TeV for $n = 2$ and 2.3 TeV for $n = 4$ to 2.0 TeV for $n = 6$, significantly extending previous results.

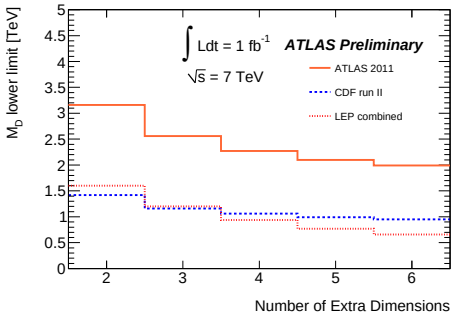

Fig. 3. The 95% CL observed lower limits on M_D for different numbers of extra dimensions for ATLAS, compared with previous results.

5 Summary and conclusions

In this note we have presented preliminary results on the search for new phenomena in an event sample with monojets and large missing transverse momentum in the final state, based on 1.00 fb^{-1} of data collected by the ATLAS experiment in 2011. Good agreement is observed between the data and the Standard Model predictions. The results are translated into model-independent 95% confidence level upper limits on fiducial cross sections that vary between 2.02 pb and 0.045 pb for the LowPt and veryHighPt analysis, respectively. The results are also interpreted in terms of the ADD LED scenario for which M_D values between 3.2 TeV and 2.0 TeV are excluded at the 95% confidence level for a number of extra dimensions varying from 2 to 6, respectively. These results significantly improve previous limits on models with Large Extra Dimensions.

References

1. The ATLAS Collaboration, ATLAS-CONF-2011-096.
2. N. Arkani-Hamed, S. Dimopoulos and G.R. Dvali, Phys. Lett. **B429** 263 (1998).
3. The ATLAS Collaboration, Phys. Lett. B**705** 294 (2011).